

## PHYSIOLOGICAL STRESS

# Physiological costs of undocumented human migration across the southern United States border

Shane C. Campbell-Staton<sup>1,2,3,\*</sup>†, Reena H. Walker<sup>4</sup>†, Savannah A. Rogers<sup>5</sup>††, Jason De León<sup>6\*</sup>, Hannah Landecker<sup>2,7</sup>, Warren Porter<sup>8</sup>, Paul D. Mathewson<sup>8</sup>, Ryan A. Long<sup>4,\*</sup>

Political, economic, and climatic upheaval can result in mass human migration across extreme terrain in search of more humane living conditions, exposing migrants to environments that challenge human tolerance. An empirical understanding of the biological stresses associated with these migrations will play a key role in the development of social, political, and medical strategies for alleviating adverse effects and risk of death. We model physiological stress associated with undocumented migration across a commonly traversed section of the southern border of the United States and find that locations of migrant death are disproportionately clustered within regions of greatest predicted physiological stress (evaporative water loss). Minimum values of estimated evaporative water loss were sufficient to cause severe dehydration and associated proximate causes of mortality. Integration of future climate predictions into models increased predicted physiological costs of migration by up to 34.1% over the next 30 years.

“You need to put yourself into the most difficult places that you can where [Border Patrol] can’t get to. You understand? Where there are lots of trees, mountains, rocks...off the trail. That’s where you need to go. If you walk in the easiest places, they will catch you quick.”

—Lucho, 47-year-old migrant from Jalisco, Mexico, interviewed June 2009 [(1), p. 189]

In 1994, the US Border Patrol adopted the border enforcement strategy referred to as Prevention Through Deterrence. This policy sought to dissuade undocumented entry across the southwest border of the United States by fortifying official ports of entry and their surrounding areas for the purpose of redirecting migrants toward more remote regions, including areas of the Chihuahuan and Sonoran Deserts (1, 2). Desert environments are among the most extreme biomes on the planet and are characterized by high maximum temperatures, large daily thermal fluctuations, and minimal water availability, which challenge biological function. In the decades since the implementation of Prevention Through

Deterrence, thousands of migrants have perished in the desert while attempting to circumvent border protection efforts (354.8 ± 71.07 deaths/year; 7805 total reported deaths from 1998 to 2019; data S1), with many more

deaths likely unreported (3). Interviews with surviving migrants depict experiences of extreme thermohydric stress—dehydration, disorientation, and organ failure—as common elements of the migrant journey:

“We were dying of thirst. I was hallucinating at that point. We were surrounded by dirt but I kept seeing water everywhere in the desert.”

—Lucho, 47-year-old migrant from Jalisco, Mexico, interviewed June 2009 [(1), p. 193]

“They abandoned me on the mountains. I didn’t have food; I didn’t have any water... [Our smuggler] abandoned us... He left us without food or water. I felt like I was almost dead. I was drinking my urine and trying to eat cactus. I am doing this for my children.”

—Monica, 27-year-old migrant from Mexico, interviewed May 2013 by J.D.L.

Although the southwest border accounts for 97.86% of total undocumented migrant

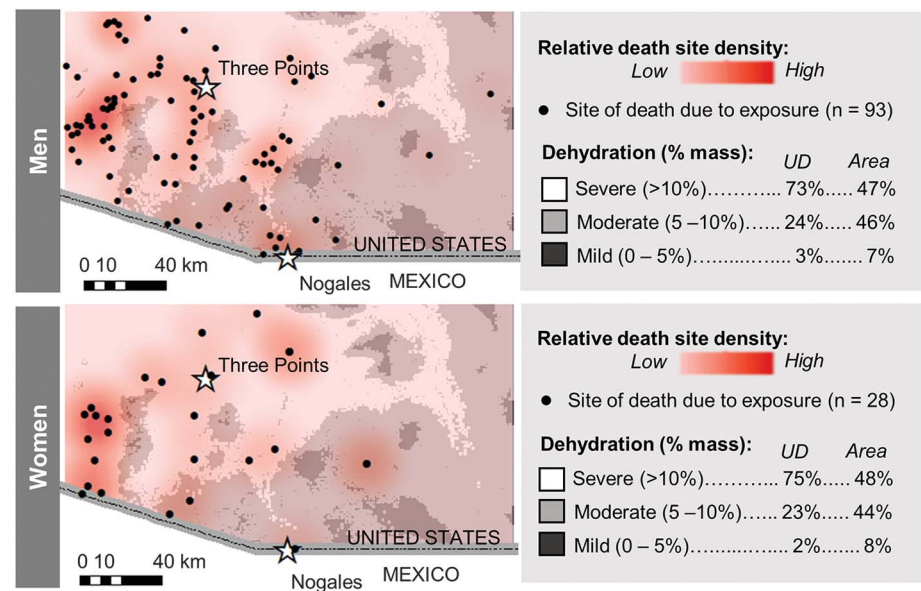


**Fig. 1. Spatial relationship between density of migrant death sites and severity of thermohydric costs.**

Utilization distributions (red scale bar) of adult male (top) and female (bottom) migrant death sites due to exposure overlaid on a spatiotemporally explicit map of the predicted costs (clinical dehydration level as percentage of body mass lost per day through evaporative water loss; gray scale bar) of traveling on foot during June in southern Arizona. Nogales and Three Points are denoted by white stars. Georeferenced migrant death sites (black dots; men, n = 93; women, n = 28) were extracted from Arizona’s OpenGIS Initiative for Deceased Migrants database (21). Only sites with known sex, age (>18 years old), cause of death (exposure), and month of death (May to September) are included. Red shading depicts the volume of the utilization distribution (95% fixed kernel); darker red indicates areas of greater kernel density volume (i.e., where more deaths occurred). Locations predicted to induce severe dehydration (>10% body mass deficit through evaporative water loss) in June are mapped in white, moderate dehydration (5 to 10% body mass deficit) in light gray, and mild dehydration (0 to 5% body mass deficit) in dark gray (22–24). The geographic distributions of male and female deaths were disproportionately concentrated in regions predicted to induce severe dehydration. See figs. S1 and S2 for results from all months.

<sup>1</sup>Department of Ecology and Evolutionary Biology, Princeton University, Princeton, NJ, USA. <sup>2</sup>Department of Ecology and Evolutionary Biology, University of California, Los Angeles, CA, USA. <sup>3</sup>Institute for Society and Genetics, University of California, Los Angeles, CA, USA. <sup>4</sup>Department of Fish and Wildlife Sciences, University of Idaho, Moscow, ID, USA. <sup>5</sup>Bioinformatics and Computational Biology, University of Idaho, Moscow, ID, USA. <sup>6</sup>Department of Anthropology and Chicana, Chicano, and Central American Studies, University of California, Los Angeles, CA, USA. <sup>7</sup>Sociology Department, University of California, Los Angeles, CA, USA. <sup>8</sup>Department of Integrative Biology, University of Wisconsin, Madison, WI, USA.

\*Corresponding author. Email: scampbellstaton@princeton.edu (S.C.C.-S.); ralong@uidaho.edu (R.A.L.); jdeleon@ucla.edu (J.D.L.)

†These authors contributed equally to this work.

‡Present address: Centre for Research into Ecological and Environmental Modelling, University of St. Andrews, St. Andrews, UK.

apprehensions in the United States each year (2000–2019; data S2), the physiological challenges faced by humans attempting to traverse the desert terrain along southern migration routes remain largely unstudied [however, see (4, 5)]. In contemporary society, causes of preventable human death are typically subject to extensive research. Yet unverified assumptions about heat stress and water loss as contributors to undocumented migrant mortality have greatly outpaced empirical work. Ethnographic insights can be synergistically coupled with physiological modeling to better understand how the extremes of the desert environment affect migrant physiology and risk of mortality. In this study, we model the physiological costs of undocumented migration across a portion of the Tucson Sector, a Border Patrol jurisdiction that runs from Yuma, Arizona, to the New Mexico border. Arizona contains 46.9% of the total primary barrier mileage (pedestrian and vehicle) across the southwest border (data S3), and the Tucson Sector, which has been a primary crossing point for migrants for nearly two decades, is characterized by the

highest number of known border-crossing fatalities (1).

To gain a clearer understanding of human physiological stress in the face of desert migration, we integrated migrant interview data with data on human physiology, morphology, and fine-scale climatic variation to parameterize a spatiotemporally explicit biophysical model, Niche Mapper (6). Niche Mapper is based on fundamental principles of heat and mass exchange between a model organism and its environment and solves the energy-balance equation using two submodels that integrate detailed data about the organism and the microclimate of its environment (6–9). Model outputs include estimated rates of metabolism and/or evaporative water loss necessary for maintaining homeothermy in the modeled environment. We used this model to simulate the physiological costs of migration by estimating rates of evaporative water loss necessary for humans to maintain heat balance while traveling by foot across the desert between Nogales, Mexico, and Three Points, Arizona (1, 2, 4).

Age, body size, sex, and reproductive status can have substantial impacts on the costs of thermoregulation (10–12), and several studies have reported a sex bias among migrants, with men being more likely to migrate than women (13, 14). More recent data, however, have shown marked increases in the number of family units and unaccompanied minors ( $\leq 17$  years old) apprehended along the southwest border (net increases for 2013–2019 for family units of +3189%, 14,855 to 473,682; and for unaccompanied minors of +196%, 38,759 to 76,020; data S4 and S5). Therefore, we used literature-derived, region-specific values of average body mass and physiological parameters to model four demographics representative of humans attempting to cross the southern US border: (i) a Latin American adult man (60.3 kg), (ii) a nonpregnant Latin American adult woman (57.7 kg), (iii) a 5-year-old Latin American child (19 kg), and (iv) a pregnant Latin American adult woman. [We estimated the costs of migrating during pregnancy by adding the average weight gain reported at 30 weeks of pregnancy (11.3 kg) to the weight of the modeled woman and adjusting physiological parameters to reflect changes due to pregnancy (15–19).] We validated our model predictions using a combination of published literature on human physiology and metabolic chamber simulations (19).

We used Niche Mapper to generate spatiotemporally explicit maps of predicted evaporative water loss in our study area (9, 20). We then evaluated how geographic variation in evaporative water loss during summer (May to September), when most migrant deaths occur (21), influenced the distribution of migrant deaths due to exposure. We compiled georeferenced records of adult ( $>18$  years old) male ( $n = 292$ ) and female ( $n = 101$ ) migrant deaths from Arizona's OpenGIS Initiative for Deceased Migrants database [1981–2019,  $n = 3251$  (21)]. We then partitioned those records by the summer month in which each death occurred. Next, we estimated 95% fixed-kernel utilization distributions (UDs) of migrant deaths due to exposure in each month and calculated the proportion of the volume of each UD that fell within each of three categories of dehydration: mild (0 to 5% body mass lost per day through evaporative water loss), medium (5 to 10% body mass lost per day), or severe ( $>10\%$  body mass lost per day) (22–24). Relative differences in costs across space and time were our primary interest in this analysis, and we assumed no water replacement.

The geographic distribution of adult male deaths from exposure was disproportionately concentrated in regions predicted to induce severe or moderate dehydration (i.e., regions with high predicted evaporative water loss) in all summer months ( $P < 0.05$  in all monthly

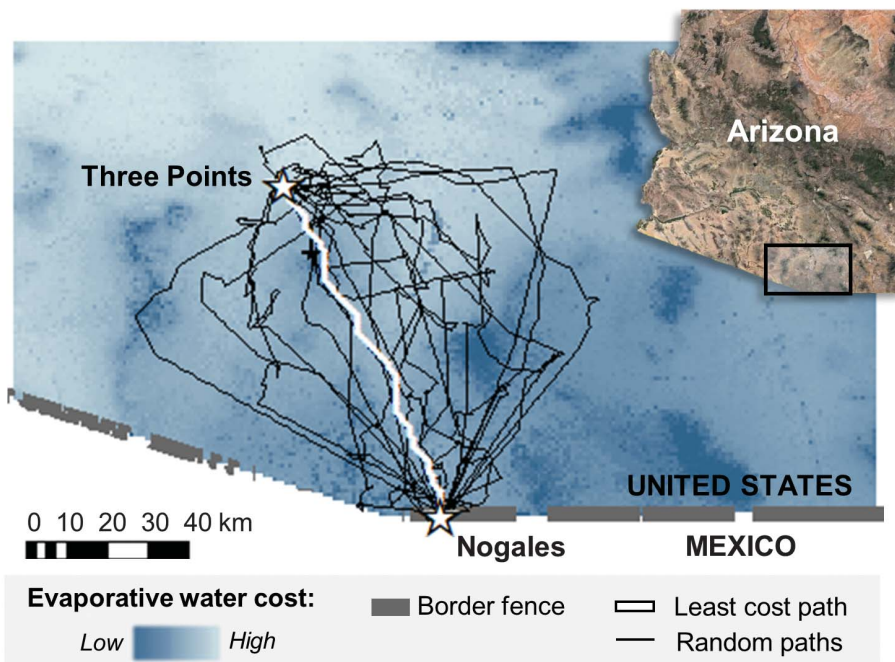


**Fig. 2. Potential migration paths between Nogales and Three Points relative to spatial variation in thermohydric costs.** Spatial variation in predicted physiological costs (evaporative water loss, liters/day) incurred by undocumented migrants at the southern US border, with least-cost and random paths used to calculate the distribution of estimated water loss incurred by migrants walking between Nogales and Three Points overlaid. The two cities lie on opposite sides of the border between the United States and Mexico, much of which is blocked by a border fence (thick gray lines) that physically separates the two countries (50). Random paths (black lines) and the least-cost path (white line) between Nogales and Three Points are overlaid on a raster (800-m resolution) that shows the predicted rate of evaporative water loss across the study area for an adult man traveling on foot during daytime hours in June. Paths were used to quantify the distribution of potential water costs for each combination of modeled individual (man, nonpregnant woman, pregnant woman, child), activity pattern (diurnal, nocturnal), departure time, and summer month (May to September). Satellite imagery for Arizona was adapted from Google Earth Pro (51). Methods for extracting spatiotemporally explicit water costs along paths are outlined in fig. S7. Results for all demographics are presented in figs. S8 to S11.

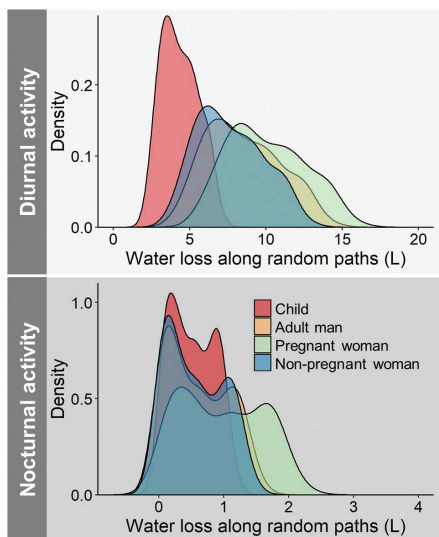


**Fig. 3. Water-loss distributions for migrants traveling along random paths between Nogales and Three Points.**

Distribution of predicted water costs for diurnal (top) versus nocturnal (bottom) travel by four migrant demographics traversing random paths ( $n = 20$ ) between Nogales and Three Points during summer (May to September). We used a custom algorithm [associated R package: *atob* (28)] to generate random trajectories (i.e., paths) at discrete time steps (15-min-step time interval) between an origin (Nogales) and destination (Three Points) using maximum travel speed, total travel time, minimum spatial resolution, and the desired number of routes as user-supplied parameters (19). We calculated total water loss along each random path by overlaying paths on spatio-temporally explicit rasters of predicted evaporative water loss for each combination of demographic, activity pattern, departure time, and month, summing the cell-specific evaporative water loss estimates along the path and multiplying the hour-specific rate of water loss in the cell (liters/s) by the time spent in the cell (s) given the modeled migrants' time of departure and movement speed (see materials and methods for a detailed description of this analysis). Diurnal travel produced substantially higher and more variable rates of water loss than nocturnal travel for all migrant demographics.

comparisons, equality of proportions test; Fig. 1 and fig. S1). By contrast, adult male deaths were either underrepresented ( $P < 0.05$ ) or proportionally represented ( $P > 0.05$ ) within regions that were predicted to induce only mild dehydration (i.e., low predicted evaporative water loss) during each month. Geographic clustering of adult female migrant deaths followed the same pattern; death sites were overrepresented in regions predicted to induce severe or moderate dehydration in all summer months ( $P < 0.05$  in all monthly comparisons, equality of proportions test) but were underrepresented or proportionally rep-

resented in areas of mild predicted dehydration (Fig. 1 and fig. S2).

Owing to the vast expanse and remoteness of the Arizona desert, many migrant deaths in this region likely go unreported (3). Among those bodies that are discovered, many are located by accident, and, as of now, there is no concerted effort at the state or federal levels to systematically retrieve bodies across the region (25). Animal scavenging and harsh environmental conditions lead to rapid decomposition and scattering of remains, decreasing the likelihood of discovery while obscuring identification and cause of death (3). Although it is often assumed that such deaths are caused by exposure, little empirical data exist regarding how physiological stress may relate to broader geographic patterns of undocumented migrant death throughout the study area.

Thus, we repeated the analysis described above using sites of migrant death for which the cause and timing of death was uncertain (adult males:  $n = 156$ ; adult females:  $n = 37$ ; fig S3). We averaged estimates of evaporative water loss across all summer months to account for uncertainty in the estimated time of death. Similar to our previous results, we found that deaths of uncertain cause among both adult men and women were disproportionately clustered within regions predicted to induce severe dehydration ( $P < 0.05$  in both comparisons, equality of proportions test; fig. S3) but were significantly underrepresented within areas of moderate and mild dehydration ( $P < 0.05$  in both comparisons, equality of proportions test; fig. S3). Though it is difficult to determine the exact proportion of these deaths that were directly due to dehydration and thermohydric stress, the significant correlation between high levels of predicted evaporative water loss and the density of deaths (indicated by the volume of the UD; figs. S4 to S6) strongly implicate temperature and water availability as major contributors to broader patterns of migrant mortality during summer.

To estimate the minimum water requirements associated with travel from Nogales to Three Points, we calculated least-cost paths for each modeled individual (man, nonpregnant woman, pregnant woman, child) during each summer month using evaporative water loss and terrain slope as equally weighted cost factors (19). In addition, because time of day affects costs of thermoregulation (26), we modeled least-cost paths under both diurnal and nocturnal activity scenarios. To quantify the cost of traveling along least-cost paths in each modeled scenario (i.e., each combination of migrant demographic, activity pattern, departure time, and month), we (i) extracted the hour-specific evaporative water-loss estimate for each raster cell intersecting the path, (ii) calculated the cell-specific evaporative

water loss (liter) by multiplying the hour-specific rate of water loss in the cell (liters/s) by the time spent in the cell (s) given the migrants' time of departure and movement speed, and (iii) summed the cell-specific costs accrued along the path (fig. S7). To capture the full distribution of evaporative water loss along each path, we calculated the cost of traversing the path using all possible hourly start times for both diurnal and nocturnal travel (19). Personal accounts of individual journeys across this landscape suggest that in many instances, migrants do not have the knowledge to identify a least-cost path of travel and may instead wander through the desert with little information about the terrain:

“[We were] in the mountains going up and down, up and down...everybody couldn't take it so the guide abandoned them. I also couldn't take it anymore. I tried again and my toenails fell off. All of these nails came off before. All of them fell off. All of them.”  
—Maria, 30-year-old migrant from Oaxaca, Mexico, interviewed May 2013 by J.D.L.

“When I was walking the last day, I felt like I was already there. I [hallucinated] a lot of things. The last hours, to get to where they were going to pick us up, I didn't see anything. Everything was spinning. I was dehydrated - I don't know what! It hurt here, in my chest.”  
—Yoanna, 27-year-old migrant from Puebla, Mexico, interviewed May 2013 by J.D.L.

Therefore, we also generated random paths of migration between Nogales and Three Points using a custom random trajectory algorithm [ $n = 20$  paths per modeled individual per month; Fig. 2; *atob* package (v0.0.0.9000) in program R (v3.5.3) (27–29)]. By combining elements of random walks and Brownian bridge movement models, the algorithm allowed us to calculate random trajectories between an origin and a destination given a user-supplied time budget for 2 days of travel (a “best-case” scenario based on ethnographic interview data), a maximum movement speed of 1.2 m/s, and a step length (i.e., distance between successive locations along the path) of 800 m (19). We quantified the cost of traversing random paths in each modeled scenario following the procedure described for least-cost paths [fig. S7; (19)].

Predicted evaporative water loss differed significantly among months and times of day for all migrant demographics. The cost (cumulative evaporative water loss) of traveling along least-cost paths ranged from 0.01 liters (the minimum for all demographics) when traveling only at night in May to 11.9 liters for a

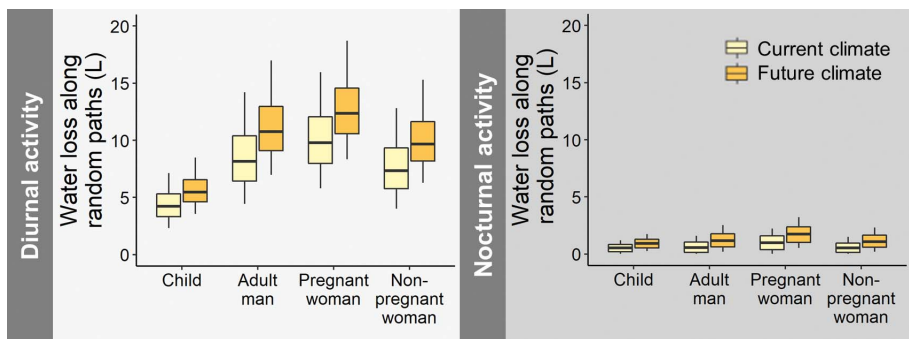


**Fig. 4. Predicted costs of migration under current versus future climate scenarios.** Distribution of predicted water costs for diurnal (left) versus nocturnal (right) travel by four migrant demographics traversing random paths ( $n = 20$ ) between Nogales and Three Points during summer (May to September) based on previous 30-year monthly average temperatures (“current climate”) and locally downscaled climate projections of temperature change over the next 30 years (“future climate”). Pixel-specific values for future climate conditions were averaged across six publicly available, locally downscaled climate models (ACCESS-1, CanESM2, CCSM4, CNRM-CM5, CSIRO-Mk3, INM-CM4) that projected monthly maximum and minimum temperatures in 2050 under RCP 4.5 (i.e., the intermediate mitigation scenario) (47, 48). Predicted water costs for migration on foot across the southern border increase significantly under this climate-change scenario relative to current conditions for all modeled migrant demographics (linear mixed-effects model,  $P < 0.001$ , Wald test). Boxes and whiskers represent median, interquartile range, and range of predicted water loss.

pregnant woman traveling during the day in June (figs. S8 to S11). Costs of traveling along more realistic, random paths were considerably higher (mean  $\pm$  SD:  $2.27 \pm 0.003$  liters higher for random paths across all scenarios). Predicted evaporative water loss peaked in June for all demographics regardless of the time of activity (linear mixed-effects model:  $P < 0.001$ , Wald test; figs. S8 to S11). Within each month, it was significantly more costly to travel during the day than at night (linear mixed-effects model:  $P < 0.001$ , Wald test; figs. S8 to S11). The distribution of thermohydric costs incurred during ~48 hours of travel from Nogales to Three Points along random paths was strongly dependent on body size, sex, and reproductive status (Fig. 3). Estimated costs of traveling at night ranged from  $0.69 \pm 0.49$  liters (mean  $\pm$  SD) for a child to  $1.29 \pm 0.92$  liters for a pregnant woman (Fig. 3). The costs of daytime travel were much higher and ranged from  $4.66 \pm 1.29$  liters for a child to  $10.76 \pm 2.72$  liters for a pregnant woman (Fig. 3). In the absence of water replacement by drinking, these rates of evaporative water loss are sufficient to cause severe dehydration and a diversity of associated conditions such as renal failure, electrolyte abnormalities, uremia, and coronary and cerebral thrombosis that are likely the proximate causes of many migrant deaths (30–38).

These models reflect contemporary climate conditions, but both changes in climate and human migration are likely to drive future patterns of mortality across the desert (39). Population surveys, econometrics, and climate analyses have documented increased human migration globally in association with changing climatic conditions (40–44). Yet the physiolog-

ical costs of human migration under such conditions have received relatively little attention. As desert environments become more extreme in the coming decades (45, 46), thermohydric stress and associated risk of mortality endured by migrant populations are also likely to increase. We next modeled the physiological costs of migration (evaporative water loss) based on anticipated climate change over the next 30 years under representative concentration pathway (RCP) 4.5 (i.e., the intermediate mitigation scenario) (47). We reparameterized the microclimate submodel of Niche Mapper with monthly minimum and maximum temperatures for 2050 by averaging predictions from six locally downscaled, publicly available climate projection models across our study area: ACCESS-1, CanESM2, CCSM4, CNRM-CM5, CSIRO-Mk3, and INM-CM4 (48). We chose a 30-year time horizon to facilitate direct comparison with our contemporary climate models, which were parameterized using average temperatures from the previous 30 years (49).

Our analysis revealed a significant increase in thermohydric costs of migration for each human demographic under the future climate change projection (linear mixed-effects model,  $P < 0.001$ , Wald test; Fig. 4). Projected increases in temperature across our study area under RCP 4.5 over the next 30 years were predicted to increase the average cost of migration along random paths between Nogales and Three Points by 34.1% for an adult man ( $1.81 \pm 0.003$  liters), 34.1% for a nonpregnant adult woman ( $1.63 \pm 0.003$  liters), 33.1% for a child ( $0.94 \pm 0.001$  liters), and 29.6% for a pregnant adult woman ( $1.90 \pm 0.003$  liters). Taken together, these results indicate that undocu-

mented migration across the southwest border of the United States will become increasingly dangerous over the next 30 years, which will likely result in increased mortality of migrants.

Biophysical models such as those presented here have been previously used to understand the dynamics of thermohydric stress in nonhuman animals in ecologically relevant contexts. We present a new application of biophysical modeling to human systems, providing a methodological framework for future studies that seek to understand the impacts of past, present, and future climate on human physiology, stress, and evolution [see (19) for caveats and considerations]. Our findings demonstrate the utility of social scientific inputs to adapt these modeling tools to humans moving through extreme landscapes. We have used this approach to show that thermohydric stress is a major contributor to patterns of undocumented migrant mortality at the southern US border. Such quantitative frameworks for studying intersecting impacts of social policy and climate change on human stress and physiology will be of increasing importance as the climate warms (39), because these methods could be extended to other situations involving outdoor exertion in conditions that challenge physiological homeostasis.

#### REFERENCES AND NOTES

1. J. De León, M. Wells, *Land of Open Graves: Living and Dying on the Migrant Trail* (Univ. California Press, ed. 1, 2015).
2. R. Rubio-Goldsmith, M. McCormick, D. Martinez, I. Duarte, “The ‘Funnel Effect’ and recovered bodies of unauthorized migrants processed by the Pima County Office of the Medical Examiner, 1990–2005” (Technical Report SSRN-id3040107, Binational Migration Institute, 2006).
3. J. Beck, I. Ostericher, G. Sollish, J. De León, *J. Forensic Sci.* **60**, S11–S20 (2015).
4. G. A. Boyce, S. N. Chambers, S. Launius, *J. Migr. Hum. Secur.* **7**, 23–35 (2019).
5. J. De León, *Am. Anthropol.* **114**, 477–495 (2012).
6. W. P. Porter, J. W. Mitchell, US Patent US7155377B2 (2006).
7. P. D. Mathewson et al., *J. Ther. Biol.* **94**, (2020).
8. M. Kearney, W. Porter, *Ecol. Lett.* **12**, 334–350 (2009).
9. Y. Natori, W. P. Porter, *Ecol. Appl.* **17**, 1441–1459 (2007).
10. M. Kleiber, *Physiol. Rev.* **27**, 511–541 (1947).
11. D. Gagnon, G. P. Kenny, *J. Physiol.* **590**, 5963–5973 (2012).
12. N. Charkoudian, N. S. Stachenfeld, *Compr. Physiol.* **4**, 793–804 (2014).
13. M. Cerrutti, D. S. Massey, in *Crossing the Border: Research from the Mexican Migration Project*, J. Durand, D. S. Massey, Eds. (Russel Sage Foundation, 2004), pp. 24–26.
14. D. S. Massey, C. Capoferro, *Int. Migr. Rev.* **38**, 1075–1102 (2004).
15. S. C. Wearpole et al., *BMC Public Health* **12**, 439 (2012).
16. R. Martorell, L. K. Khan, M. L. Hughes, L. M. Grummer-Strawn, *J. Nutr.* **128**, 1464–1473 (1998).
17. P. Durán et al., *Acta Paediatr.* **105**, e116–e125 (2016).
18. K. M. Rasmussen, A. L. Yaktine, Eds., *Weight Gain During Pregnancy: Reexamining the Guidelines* (National Academies Press, 2009).
19. Materials and methods are available as supplementary materials.
20. M. R. Kearney, W. P. Porter, *Ecography* **40**, 664–674 (2017).
21. Arizona OpenGIS Initiative for Deceased Migrants, Custom map of migrant mortality (2019); <https://humaneborders.info/app/map.asp>.
22. K. E. D’Anci, F. Constant, I. H. Rosenberg, *Nutr. Rev.* **64**, 457–464 (2006).
23. World Health Organization (WHO), “The treatment of diarrhea: A manual for physicians and other senior health workers” (WHO/CDD/SER/80.2 rev. 4, WHO, 2005).
24. American Academy of Pediatrics Provisional Committee on Quality Improvement, *Pediatrics* **97**, 424–436 (1996).

25. M. Jimenez, "Humanitarian crisis: Migrant deaths at the U.S.-Mexico border" (American Civil Liberties Union, 2009).
26. W. P. Porter, *Ecol. Monogr.* **37**, 273–296 (1967).
27. G. Technitis, W. Othman, K. Safi, R. Weibel, *Int. J. Geogr. Inf. Sci.* **29**, 912–934 (2015).
28. S. Rogers, *atob*: Creates random routes between two points, GitHub (2019); <https://github.com/SavannahAlicia/atob/>.
29. R Core Team, R: A language and environment for statistical computing (R Foundation for Statistical Computing, Vienna, 2018); [www.R-project.org/](http://www.R-project.org/).
30. J. González-Alonso, R. Mora-Rodríguez, P. R. Below, E. F. Coyle, *J. Appl. Physiol.* **82**, 1229–1236 (1997).
31. H. R. Lieberman, *J. Am. Coll. Nutr.* **26**, 555S–561S (2007).
32. L. Nybo, *J. Appl. Physiol.* **104**, 871–878 (2008).
33. P. M. Clarkson, *Sports Med.* **37**, 361–363 (2007).
34. G. C. Donaldson, W. R. Keatinge, R. D. Saunders, *Int. J. Hyperthermia* **19**, 225–235 (2003).
35. C. L. Chapman *et al.*, *J. Appl. Physiol.* **128**, 715–728 (2020).
36. J. González-Alonso, C. G. Crandall, J. M. Johnson, *J. Physiol.* **586**, 45–53 (2008).
37. J. Tikkanen, O. P. Heinonen, *Eur. J. Epidemiol.* **7**, 628–635 (1991).
38. R. Boni, *Mol. Reprod. Dev.* **86**, 1307–1323 (2019).
39. H. Benveniste, M. Oppenheimer, M. Fleurbaey, *Proc. Natl. Acad. Sci. U.S.A.* **117**, 26692–26702 (2020).
40. V. Mueller, C. Gray, K. Kosec, *Nat. Clim. Chang.* **4**, 182–185 (2014).
41. A. Dillon, V. Mueller, S. Salau, *Am. J. Agric. Econ.* **93**, 1048–1061 (2011).
42. L. Marchiori, J. F. Maystadt, I. Schumacher, *J. Environ. Econ. Manage.* **63**, 355–374 (2012).
43. C. L. Gray, V. Mueller, *Proc. Natl. Acad. Sci. U.S.A.* **109**, 6000–6005 (2012).
44. T. Halliday, *Econ. Dev. Cult. Change* **54**, 893–925 (2006).
45. J. L. Weiss, J. T. Overpeck, *Glob. Change Biol.* **11**, 2065–2077 (2005).
46. S. R. Loarie *et al.*, *Nature* **462**, 1052–1055 (2009).
47. M. Collins *et al.*, in *Climate Change 2013: The Physical Science Basis. Contribution of Working Group I to the Fifth Assessment Report of the Intergovernmental Panel on Climate Change*, T. F. Stocker *et al.*, Eds. (Cambridge Univ. Press, 2013).
48. T. Wang, A. Hamann, D. Spittlehouse, C. Carroll, *PLOS ONE* **11**, e0156720 (2016).
49. C. Daly *et al.*, *Int. J. Climatol.* **28**, 2031–2064 (2008).
50. M. J. Cory, Border-fence map. Reveal from The Center for Investigative Reporting and OpenStreetMap contributors (2017); [www.arcgis.com/home/item.html?id=2aac3acce15a4b56ab483c48243880d4](http://www.arcgis.com/home/item.html?id=2aac3acce15a4b56ab483c48243880d4).
51. Google Earth Pro V.7.3.3.7786, Arizona, United States of America. 111.093731, 34.048928. Eye alt 727.17 mi. SIO, NOAA, US Navy, NGA, GEBCO, 19 January 2021.

#### ACKNOWLEDGMENTS

We acknowledge the invaluable contributions of the men, women, and children whose personal experiences and stories informed the parameters of this study. We also acknowledge the innumerable lives, both known and unknown, that have been affected by the past and ongoing circumstances that contextualize this work. This study would have been impossible without the bravery and sacrifice of these individuals. **Funding:** Infrastructure support for this

study was provided by the University of California, Los Angeles (UCLA); University of Idaho; and University of Wisconsin. **Author contributions:** S.C.C.-S. and R.A.L. conceived of and conceptualized this study. S.A.R., P.D.M., and W.P. developed the methodology described herein. R.H.W., S.A.R., P.D.M., and W.P. performed modeling and validation of the experiments performed. J.D.L. provided ethnographic data used to parameterize the models. All results were visualized by R.H.W. Supervision of experiments and their contextualization were provided by R.A.L., H.L., and J.D.L. The original draft of the manuscript was written by S.C.C.-S., H.L., and R.H.W., then reviewed and edited by S.C.C.-S., R.H.W., S.A.R., J.D.L., H.L., W.P., P.D.M., and R.A.L. **Competing interests:** The authors declare that they have no competing interests. **Data and materials availability:** All data are available in the main text and supplementary materials.

#### SUPPLEMENTARY MATERIALS

[science.org/doi/10.1126/science.abh1924](http://science.org/doi/10.1126/science.abh1924)  
Materials and Methods  
Figs. S1 to S18  
Tables S1 to S8  
References (52–115)  
MDAR Reproducibility Checklist  
Data S1 to S6

[View/request a protocol for this paper from Bio-protocol.](#)

25 February 2021; resubmitted 4 June 2021  
Accepted 21 October 2021  
10.1126/science.abh1924

## Physiological costs of undocumented human migration across the southern United States border

Shane C. Campbell-StatonReena H. WalkerSavannah A. RogersJason De LeónHannah LandeckerWarren PorterPaul D. MathewsonRyan A. Long

*Science*, 374 (6574), • DOI: 10.1126/science.abh1924

### Dangerous terrain

As climate change leads to regions of the world becoming increasingly uninhabitable, unregulated human migration is likely to increase. Migrants often traverse dangerous terrain, and the environmental conditions they encounter when exposed can be deadly. Campbell-Staton *et al.* used an approach commonly used to predict spatially explicit regions of physiological challenge in animal species to create a hazard landscape for the border crossing between the United States and Mexico. Their predictions of high risk, particularly due to dehydration, coincided with regions of high migrant mortality. Such detailed predictions may help to prevent these tragedies. —SNV

### View the article online

<https://www.science.org/doi/10.1126/science.abh1924>

### Permissions

<https://www.science.org/help/reprints-and-permissions>

Use of think article is subject to the [Terms of service](#)

---

*Science* (ISSN ) is published by the American Association for the Advancement of Science. 1200 New York Avenue NW, Washington, DC 20005. The title *Science* is a registered trademark of AAAS.

Copyright © 2021 The Authors, some rights reserved; exclusive licensee American Association for the Advancement of Science. No claim to original U.S. Government Works